# Supplementary Information

# Three angular $Zn_2Dy$ complexes showing effect of remote coordination at Zn and counter ions on the slow magnetic relaxation at Dy centre

Anangamohan Panja*[a,b] Zvonko Jagličić,[c] Paula Brandão,[d] Kuheli Pramanik [a,b] and Narayan Ch. Jana,[a]

[a] *Department of Chemistry, Panskura Banamali College, Panskura RS, WB 721152, India*

[b] *Department of Chemistry, Gokhale Memorial Girls' College, 1/1 Harish Mukherjee Road, Kolkata-700020, India.*

[c] *Institute of Mathematics, Physics and Mechanics & Faculty of Civil and Geodetic Engineering, University of Ljubljana, Jadranska 19, 1000 Ljubljana, Slovenia*

[d] *Department of Chemistry, CICECO-Aveiro Institute of Materials, University of Aveiro, 3810-193 Aveiro, Portugal*

* Corresponding author e-mail: ampanja@yahoo.co.in

**Table of Contents**

**Table S1**. Bond distances around metal coordination spheres in **1−3**

| **Bond** | **Distances** | | |
|---|---|---|---|
| | **1**[#] | **2** | **3** |
| Dy–O1 | 2.271(5) | 2.322(2) | 2.273(2) |
| Dy–O2(or O4) | 2.692(6) | 2.679(2) | 2.673(2) |
| Dy–O3 (or O12) | 2.343(6) | 2.255(2) | 2.347(2) |
| Dy–O5(or O8) | 2.370(7) | 2.324(2) | 2.354(2) |
| Zn–X (Cl/Br/I) | 2.269(2) | 2.399(1) | 2.616(1) |
| Zn–O1 | 2.030(5) | 2.034(2) | 2.024(2) |
| Zn–O3(or O12) | 2.051(5) | 2.007(1) | 2.049(2) |
| Zn–N1 | 2.099(6) | 2.043(2) | 2.084(2) |
| Zn–N2 | 2.061(7) | 2.067(2) | 2.058(2) |
| Dy···Zn | 3.493(1) | 3.460(2) | 3.494(1) |

[#] Bond distances of only one crystallographically independent complex cation are given

**Table S2**. SHAPE analysis of the Dy(III) ion for complexes **1−3**.

| Label | Shape | Symmetry | Distortion (**1**) | | Distortion (**2**) | Distortion (**3**) |
|---|---|---|---|---|---|---|
| | | | Dy1 | Dy2 | Dy1 | Dy1 |
| OP-8 | Octagon | $D_{8h}$ | 30.198 | 30.419 | 32.728 | 32.943 |
| HPY-8 | Heptagonal pyramid | $C_{7v}$ | 20.888 | 20.265 | 23.134 | 23.359 |
| HBPY-8 | Hexagonal bipyramid | $D_{6h}$ | 9.520 | 10.056 | 9.646 | 9.888 |

| | | | | | | |
|---|---|---|---|---|---|---|
| CU-8 | Cube | $O_h$ | **4.628** | **5.232** | **3.923** | **4.053** |
| SAPR-8 | Square antiprism | $D_{4d}$ | **4.547** | **4.451** | **4.303** | **3.993** |
| TDD-8 | Triangular dodecahedron | $D_{2d}$ | **3.948** | **3.774** | **4.082** | **3.870** |
| JGBF-8 | Johnson gyrobifastigium J26 | $D_{2d}$ | 13.159 | 13.081 | 13.568 | 13.542 |
| JETBPY-8 | Johnson elongated triangular bipyramid J14 | $C_{3h}$ | 23.758 | 23.879 | 24.070 | 24.342 |
| JBTPR-8 | Biaugmented trigonal prism J50 | $C_{2v}$ | 6.326 | 6.056 | 6.480 | 6.232 |
| BTPR-8 | Biaugmented trigonal prism | $C_{2v}$ | 6.292 | 6.049 | 6.406 | 6.114 |
| JSD-8 | Snub diphenoid J84 | $D_{2d}$ | 6.971 | 6.555 | 7.542 | 7.385 |
| TT-8 | Triakis tetrahedron | $T_d$ | **4.662** | **5.207** | **3.923** | **4.109** |
| ETBPY-8 | Elongated trigonal bipyramid | $D_{3h}$ | 17.997 | 17.229 | 18.682 | 18.511 |

**Table S3**. Relaxation fitting parameters from the least-square fitting of the Cole-Cole plots of **1** in the temperature range 1.9 K–10.0 K by the generalized Debye model.

| $T$ (K) | $\chi_S$ (emu/mol) | $\Delta\chi$ (emu/mol) | $\tau$ (s) | $\alpha$ |
|---|---|---|---|---|
| 1.9 | 0.35551 | 4.65656 | 0.00174 | 0.39228 |
| 2.09 | 0.31816 | 4.21951 | 0.00143 | 0.40764 |
| 2.29 | 0.33228 | 3.87446 | 0.00122 | 0.40024 |
| 2.48 | 0.34971 | 3.56489 | 0.00104 | 0.38936 |
| 2.67 | 0.37044 | 3.29147 | 8.95E-04 | 0.37728 |
| 2.87 | 0.38152 | 3.05708 | 7.71E-04 | 0.36621 |
| 3.06 | 0.39714 | 2.84116 | 6.69E-04 | 0.35638 |
| 3.25 | 0.40019 | 2.66563 | 5.78E-04 | 0.35015 |
| 3.45 | 0.40001 | 2.50865 | 4.99E-04 | 0.34642 |
| 3.64 | 0.43253 | 2.32625 | 4.43E-04 | 0.3353 |
| 3.83 | 0.40186 | 2.23298 | 3.71E-04 | 0.34367 |
| 4.03 | 0.41895 | 2.09582 | 3.27E-04 | 0.34188 |
| 4.22 | 0.41187 | 1.99915 | 2.83E-04 | 0.34685 |
| 4.42 | 0.43362 | 1.88362 | 2.55E-04 | 0.34749 |
| 4.61 | 0.44638 | 1.77849 | 2.27E-04 | 0.34723 |
| 4.8 | 0.44607 | 1.69649 | 2.01E-04 | 0.35071 |
| 5 | 0.4752 | 1.58714 | 1.83E-04 | 0.34981 |
| 5.5 | 0.52473 | 1.36045 | 1.47E-04 | 0.3481 |
| 6 | 0.54882 | 1.18664 | 1.16E-04 | 0.34969 |
| 6.5 | 0.5756 | 1.03525 | 9.69E-05 | 0.33992 |
| 7 | 0.61795 | 0.88424 | 8.36E-05 | 0.33394 |
| 7.5 | 0.63094 | 0.7758 | 7.00E-05 | 0.32766 |
| 8 | 0.67865 | 0.64245 | 6.53E-05 | 0.31186 |
| 8.5 | 0.62598 | 0.62317 | 4.38E-05 | 0.3293 |
| 9 | 0.62037 | 0.56338 | 3.53E-05 | 0.3325 |
| 9.5 | 0.49801 | 0.62674 | 1.85E-05 | 0.3577 |
| 10 | 0.33254 | 0.74001 | 8.11E-06 | 0.39487 |

**Table S4**. The splitting of $^6H_{15/2}$ the lowest multiplets for **1** calculated by CASSCF/SINGLE_ANISO together with *g*-values for each Kramers doublets

| $E$ (cm$^{-1}$) | $g_x$ | $g_y$ | $g_z$ |
|---|---|---|---|
| 0 | 0.123 | 0.267 | 19.029 |
| 108 | 0.874 | 1.434 | 15.916 |
| 164 | 1.276 | 3.224 | 12.800 |
| 224 | 3.288 | 3.986 | 9.772 |
| 283 | 0.236 | 0.973 | 18.277 |
| 346 | 2.539 | 5.330 | 8.256 |
| 412 | 1.992 | 6.389 | 13.077 |
| 614 | 0.057 | 0.155 | 19.220 |

**Table S5**. The splitting of $^6H_{15/2}$ the lowest multiplets for **2** calculated by CASSCF/SINGLE_ANISO together with *g*-values for each Kramers doublets

| $E$ (cm$^{-1}$) | $g_x$ | $g_y$ | $g_z$ |
|---|---|---|---|
| 0 | 0.072 | 0.167 | 19.224 |
| 114 | 0.624 | 0.751 | 16.521 |
| 200 | 0.857 | 1.475 | 14.829 |
| 255 | 0.458 | 2.401 | 13.754 |
| 333 | 1.039 | 2.373 | 11.553 |
| 409 | 3.069 | 5.393 | 11.696 |
| 554 | 0.630 | 0.865 | 18.468 |
| 719 | 0.063 | 0.201 | 19.428 |

**Table S6**. The splitting of $^6H_{15/2}$ the lowest multiplets for **3** calculated by CASSCF/SINGLE_ANISO together with *g*-values for each Kramers doublets

| $E$ (cm$^{-1}$) | $g_x$ | $g_y$ | $g_z$ |
|---|---|---|---|
| 0 | 0.064 | 0.132 | 19.318 |

| | | | |
|---|---|---|---|
| 117 | 0.639 | 0.812 | 16.638 |
| 183 | 0.687 | 1.363 | 15.351 |
| 223 | 0.369 | 2.205 | 14.256 |
| 292 | 1.345 | 2.588 | 11.266 |
| 366 | 3.068 | 5.245 | 11.735 |
| 509 | 0.627 | 0.848 | 18.392 |
| 655 | 0.081 | 0.262 | 19.344 |

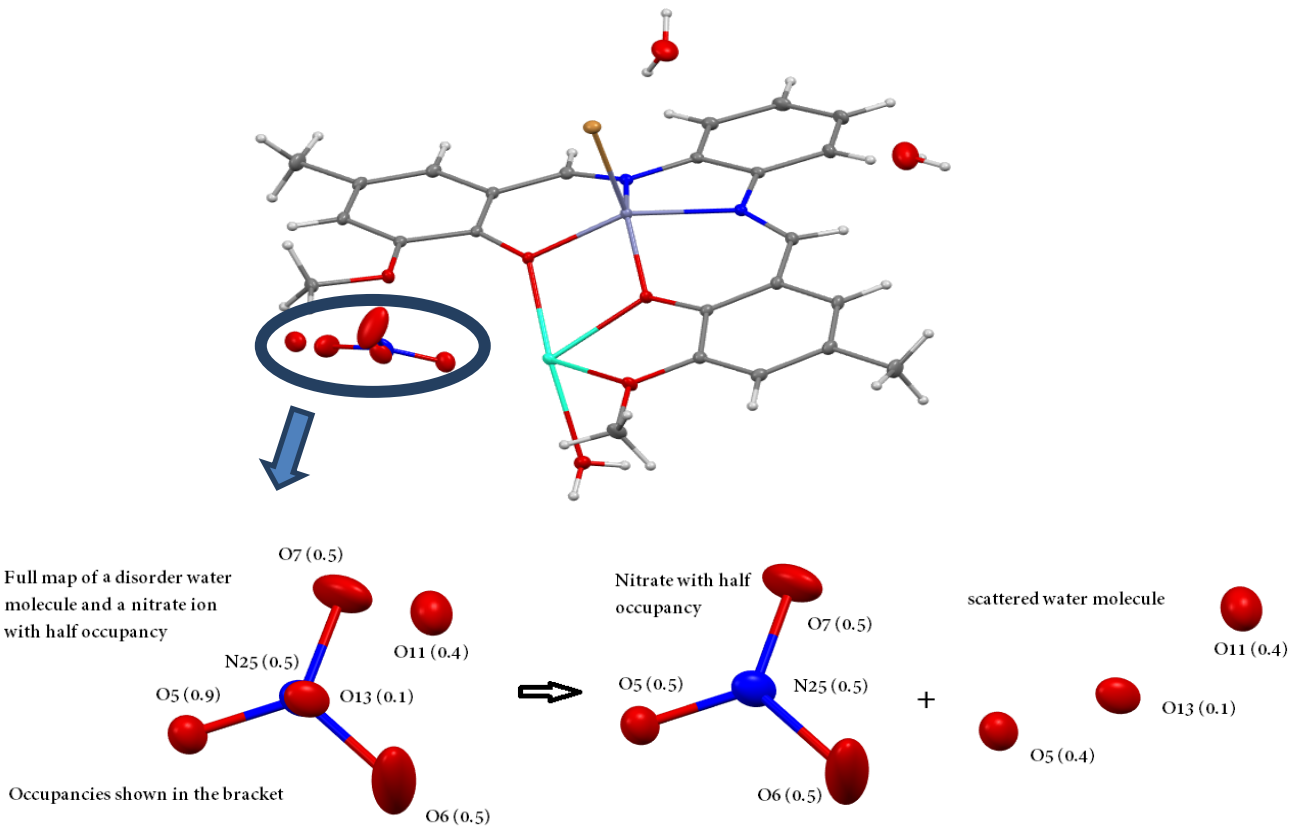


**Fig. S1.** Asymmetric unit of complex **2** displaying a nitrate ion with half occupancy together with a scatter molecule of water of crystallisation over a same region. The bottom half showing contribution of each part in the full map.

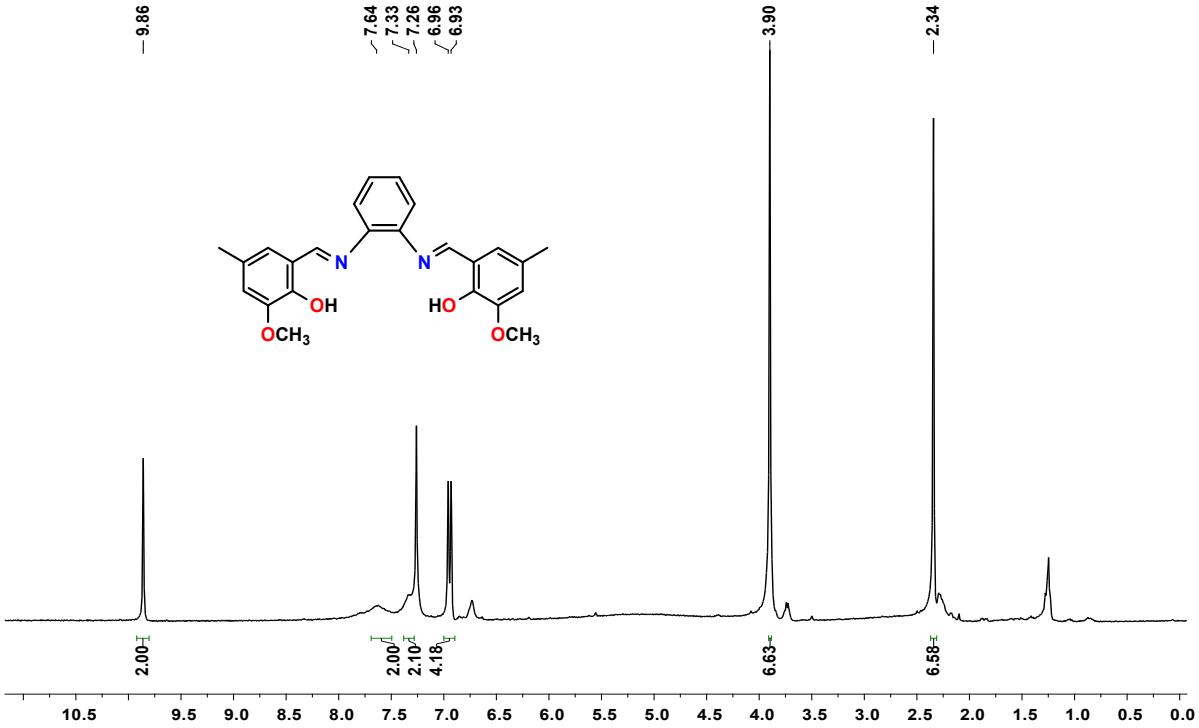


**Fig. S2.** $^{1}$H NMR of Schiff base ligand *N,N′*-bis(3-methoxy-5-methylsalicylidene)-1,2-phenylenediamine ($H_2L$) in $CDCl_3$ at r.t.

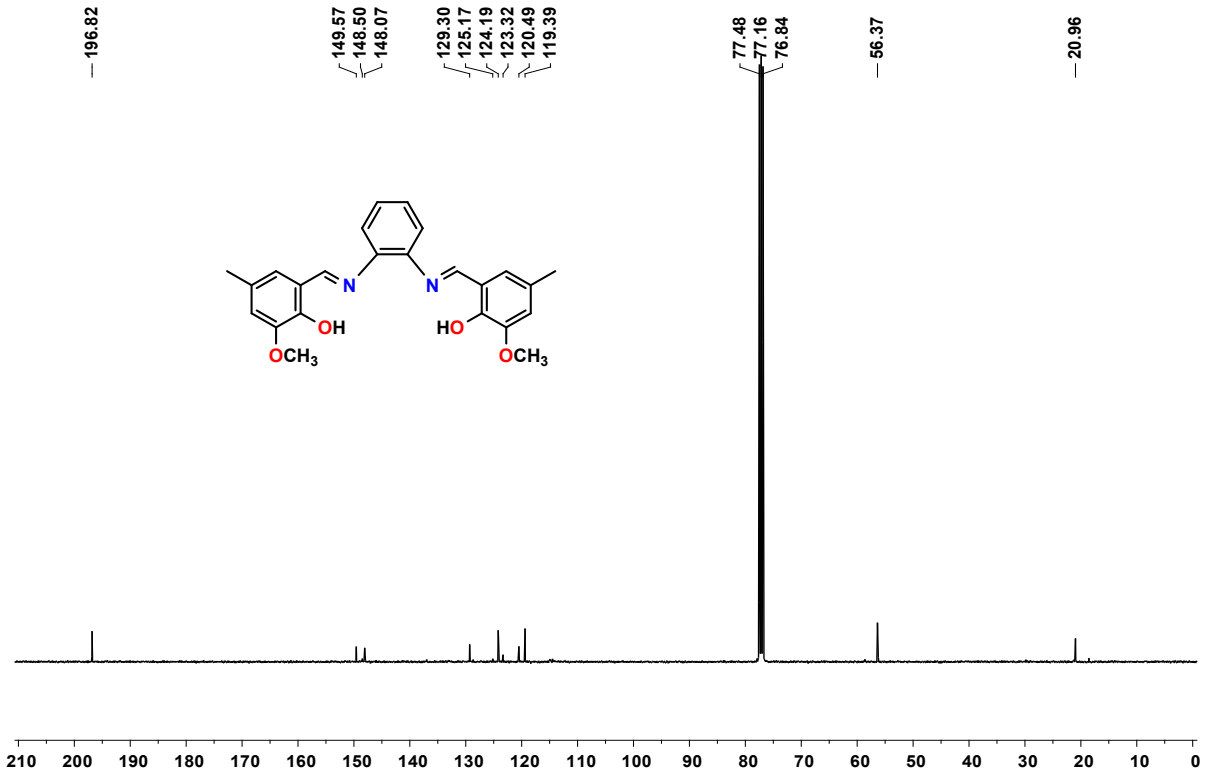

**Fig. S3**: $^{13}C$ NMR of Schiff base ligand *N,N'*-bis(3-methoxy-5-methylsalicylidene)-1,2-phenylenediamine ($H_2L$) in $CDCl_3$ at r.t.

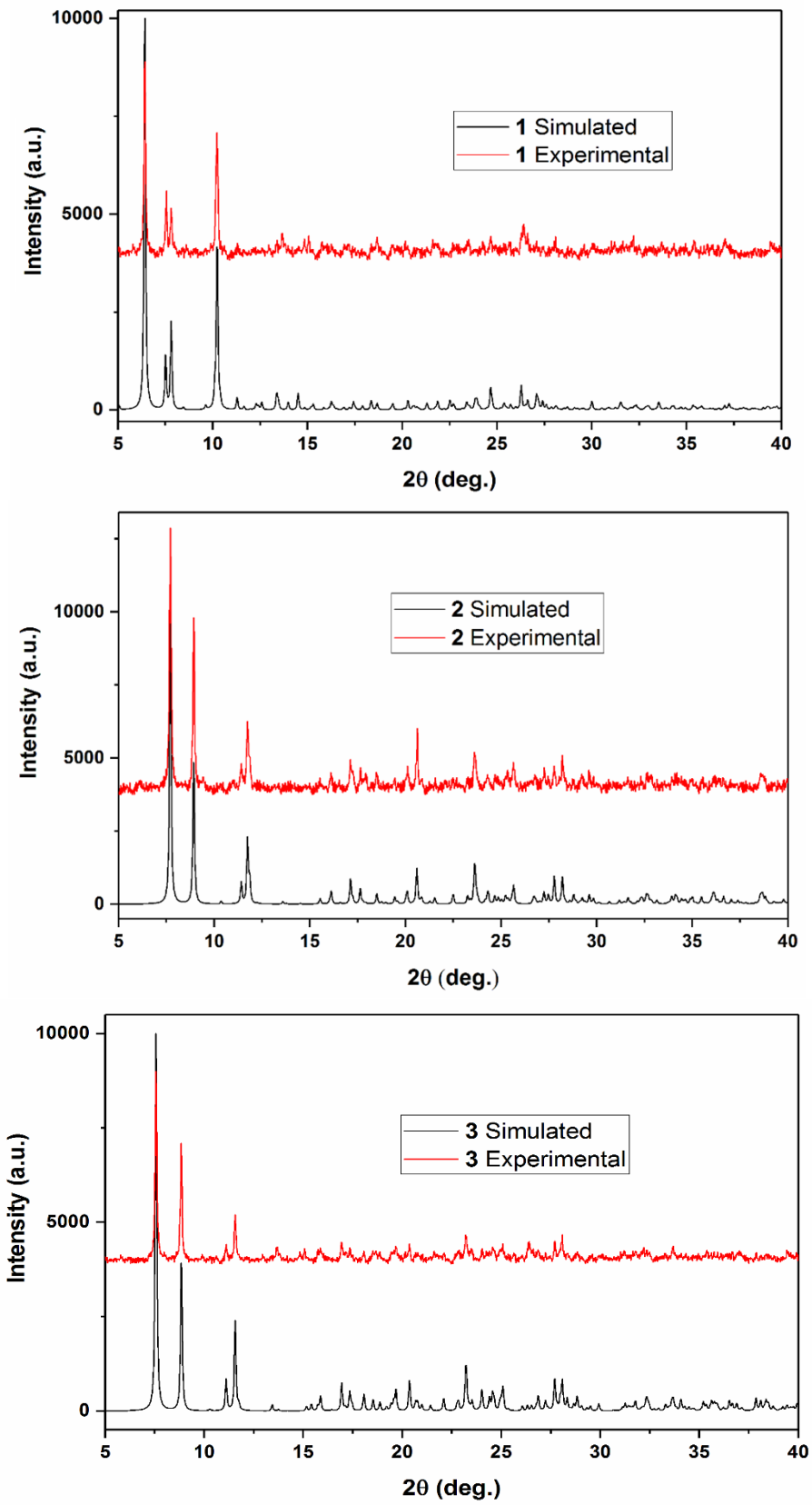

**Fig. S4**: (a), (b) and (c) represent experimental and simulated PXRD patterns of **1-3**.

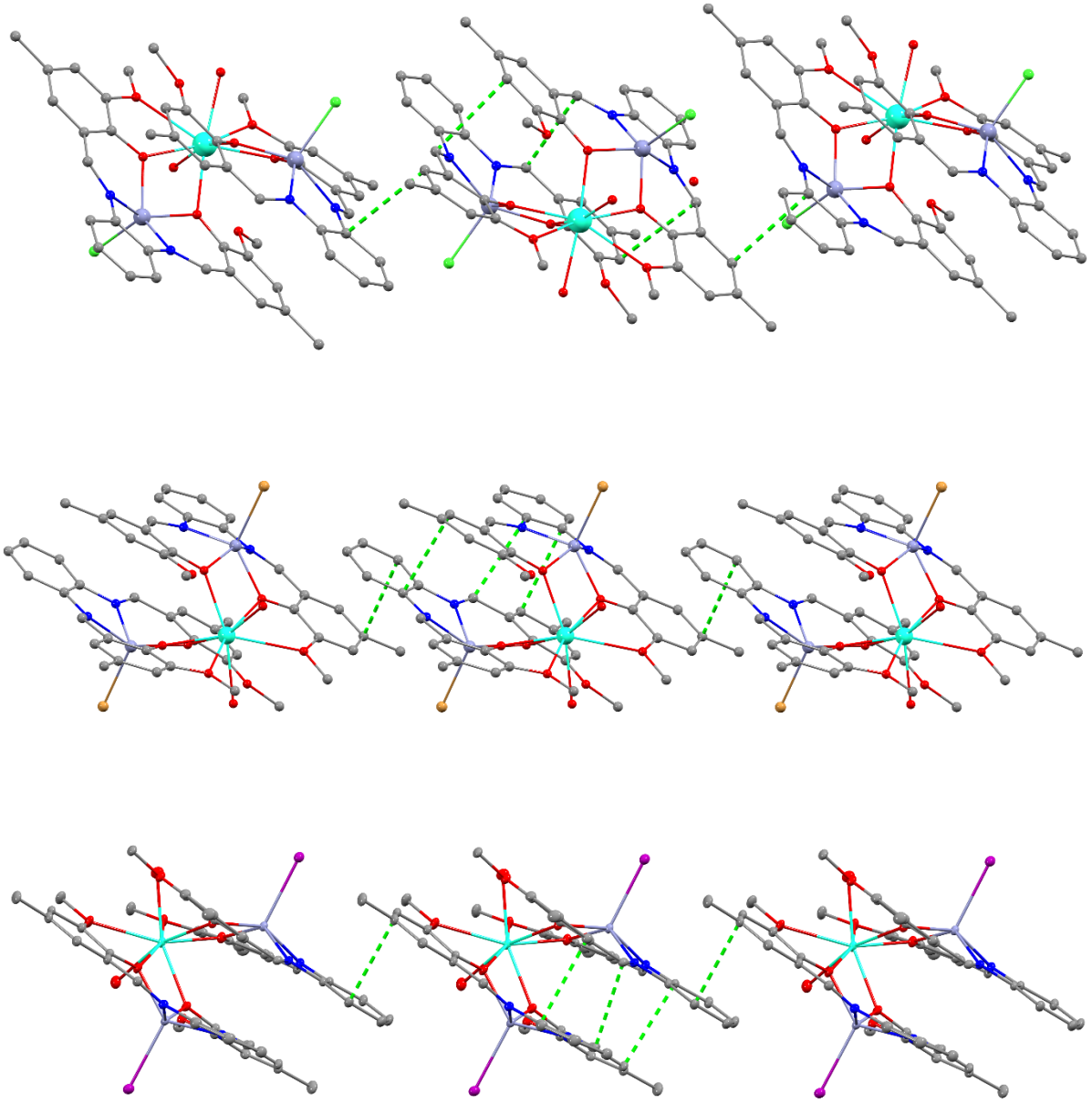

**Fig. S5**. A part of crystal packing of **1–3** showing both trimolecular and intermolecular π–π interactions.

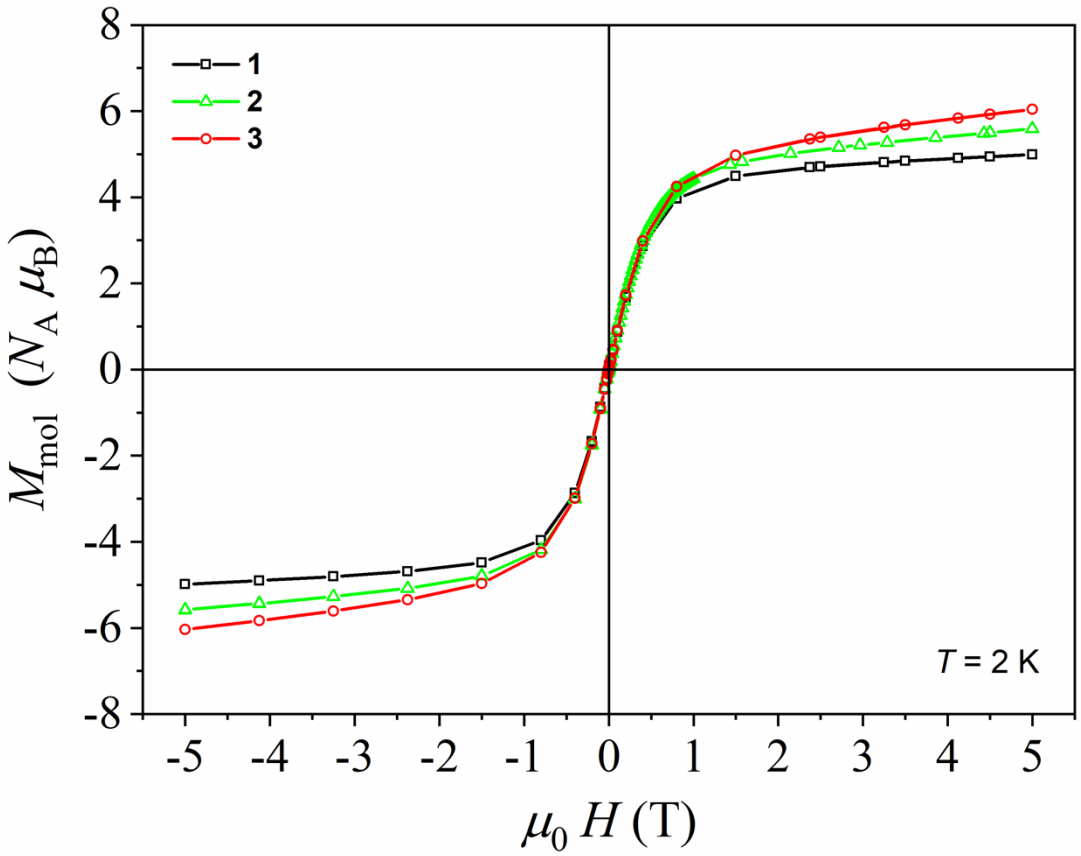


**Fig. S6**. Magnetization plots of **1–3** at 2 K.

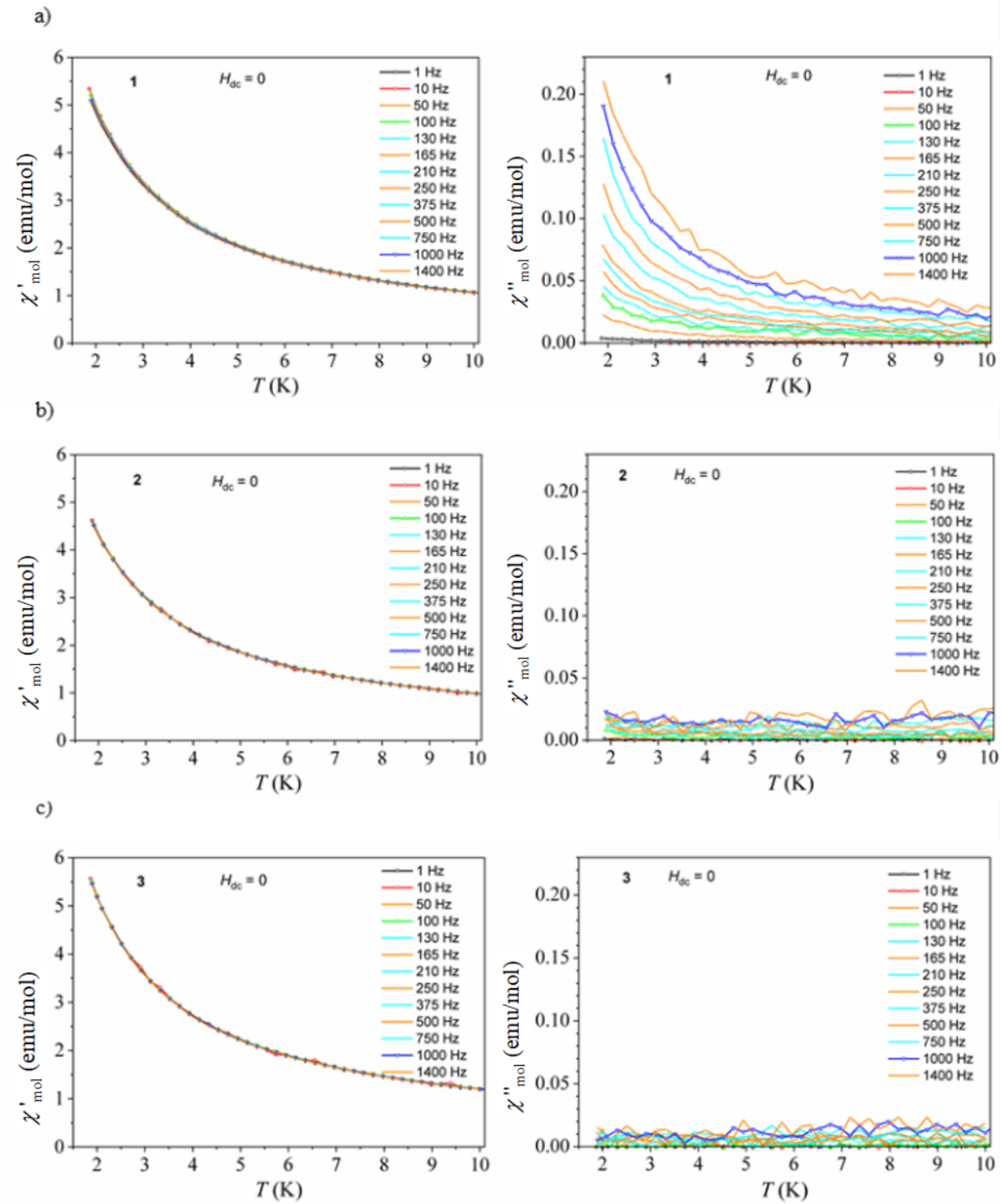


**Fig. S7**. (a) to (c) represent the real and imaginary parts of ac susceptibility in 0 kOe dc field as a function of temperature for complexes **1–3**, respectively

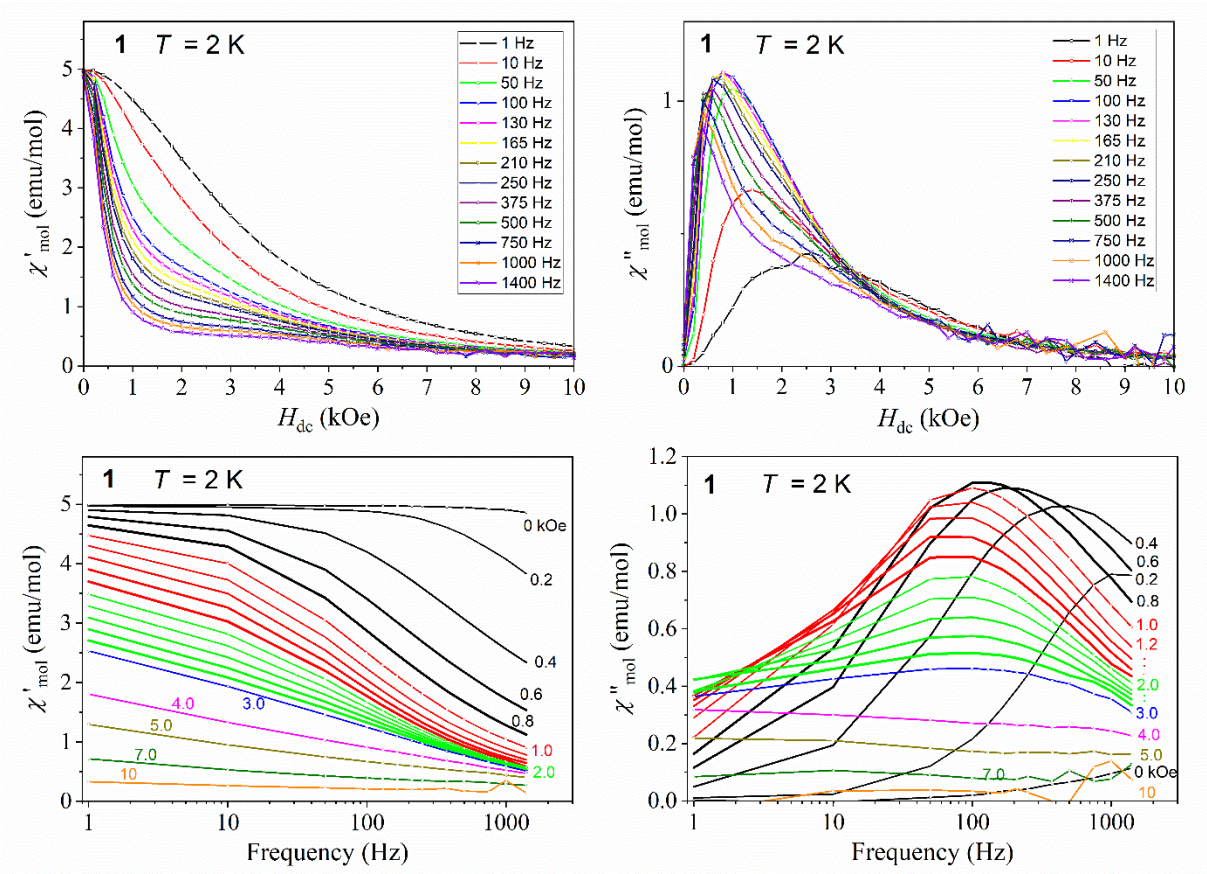


**Fig. S8**. Real and imaginary part of ac susceptibility at 2 K as a function of dc magnetic field (Top) and frequency (Bottom) for **1**.

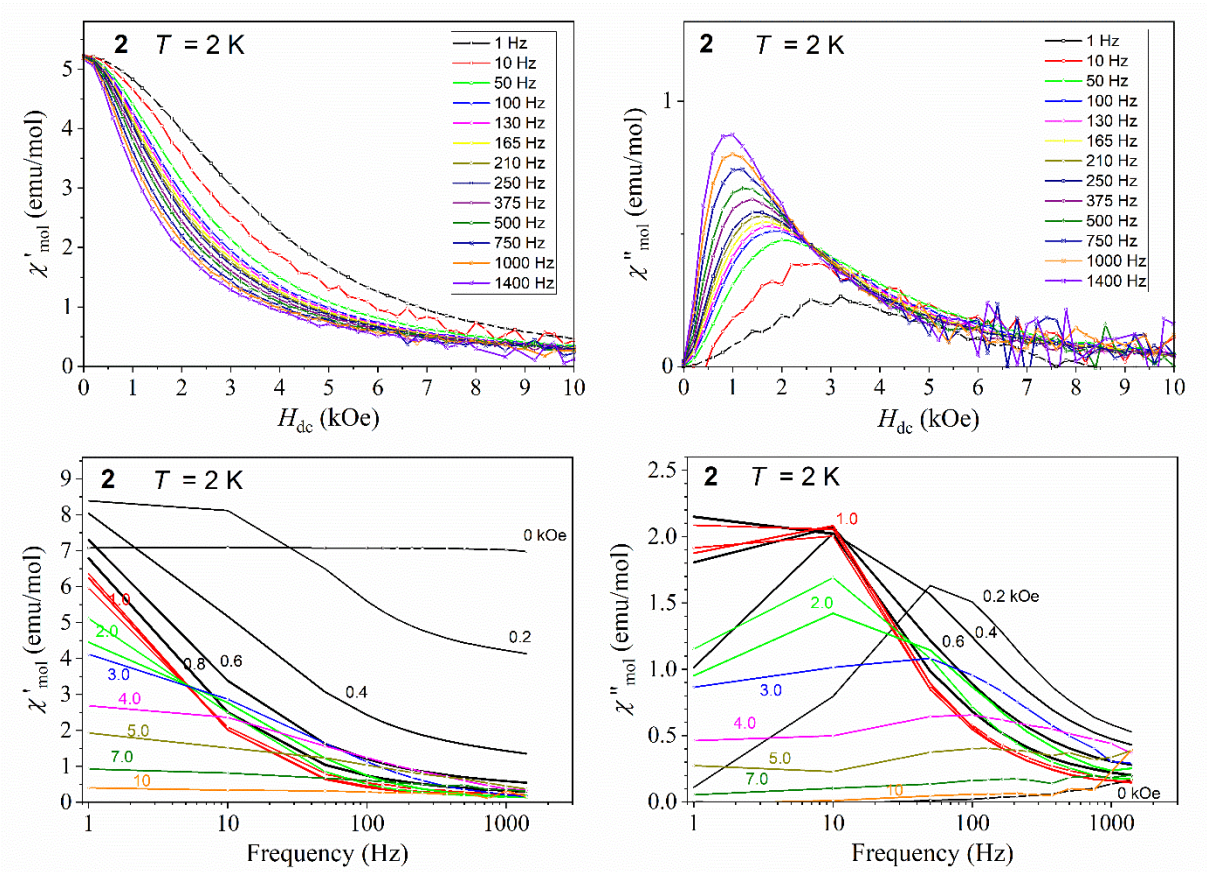


**Fig. S9**. Real and imaginary part of ac susceptibility at 2 K as a function of dc magnetic field (Top) and frequency (Bottom) for **2**.

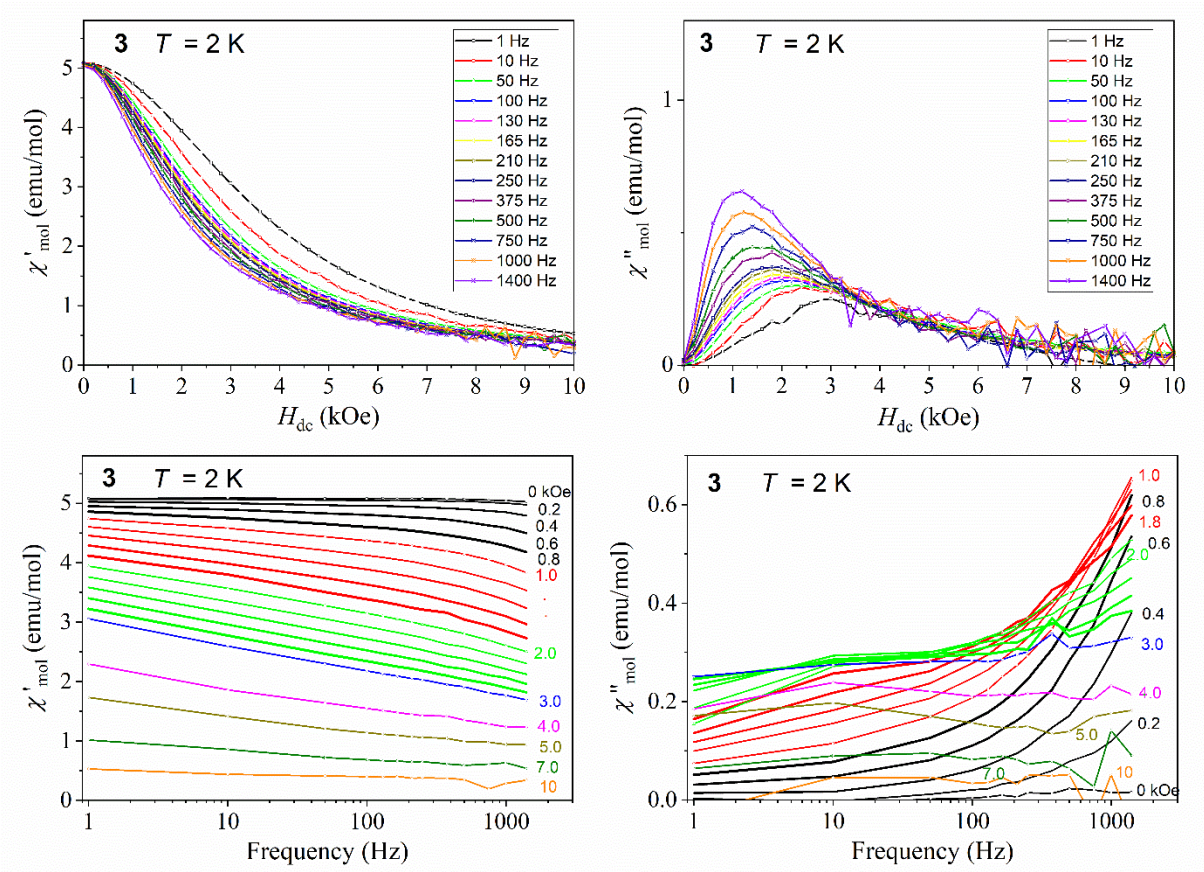


**Fig. S10**. Real and imaginary part of ac susceptibility at 2 K as a function of dc magnetic field (Top) and frequency (Bottom) for **3**.

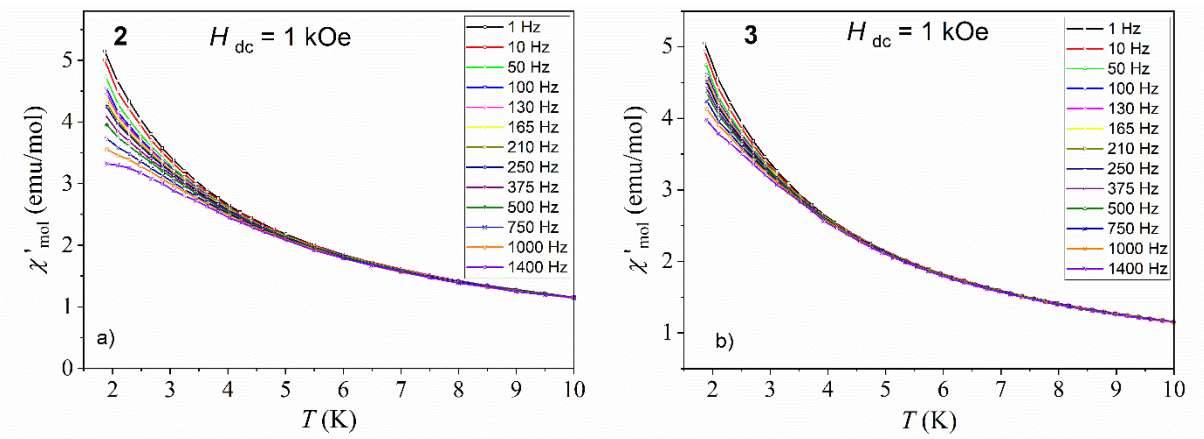


**Fig. S11**. (a) and (b) represent the temperature dependence of the in-phase ac susceptibility component of **2** and **3**, respectively, measured at 1.0 kOe applied magnetic field.

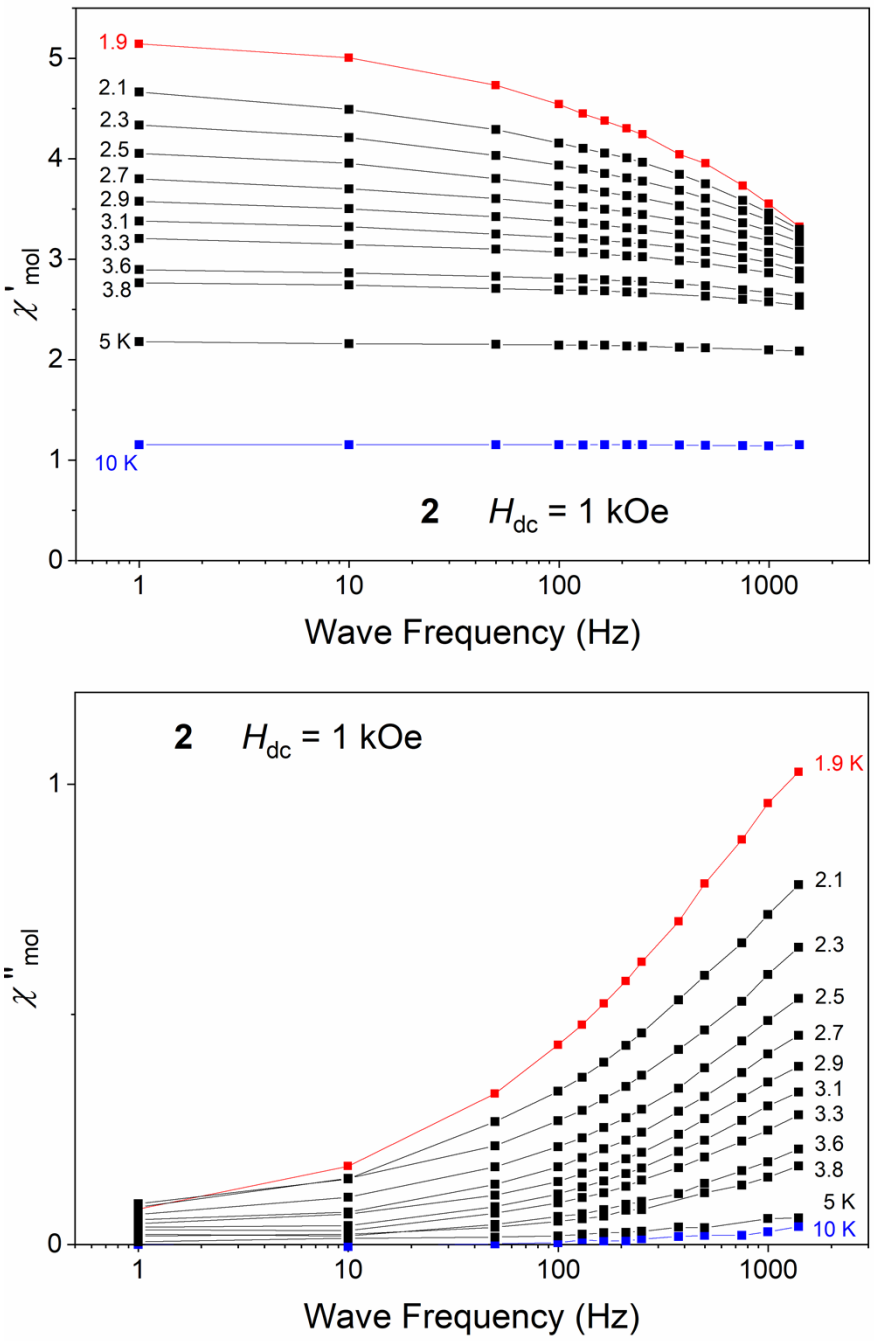


**Fig. S12**. Frequency dependence of the in-phase and out-of-phase ac susceptibility components of **2** measured in the temperature range 1.9–10 K and at 1.0 kOe applied magnetic field.

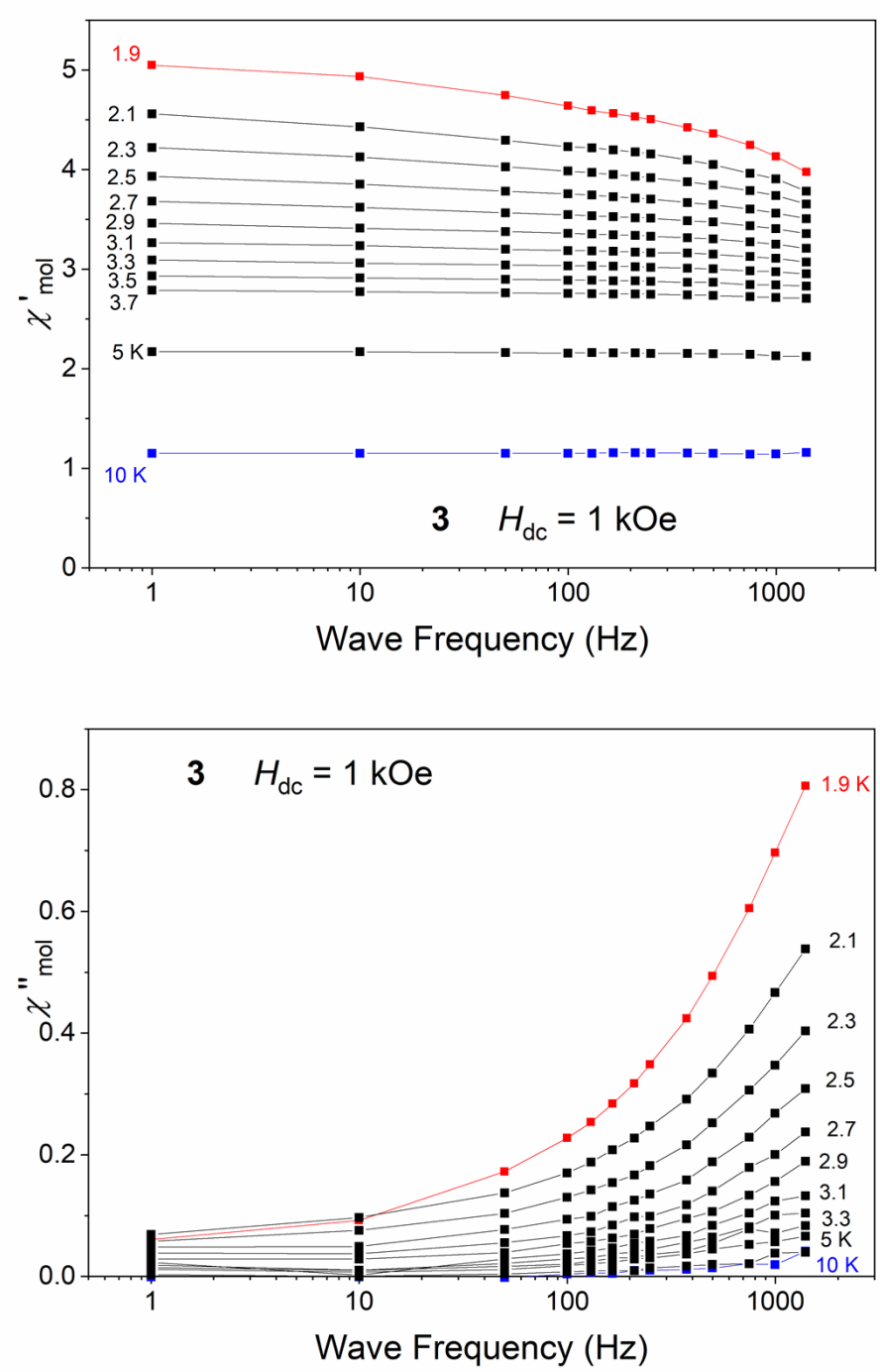


**Fig. S13**. Frequency dependence of the in-phase and out-of-phase ac susceptibility components of **3** measured in the temperature range 1.9–10 K and at 1.0 kOe applied magnetic field.

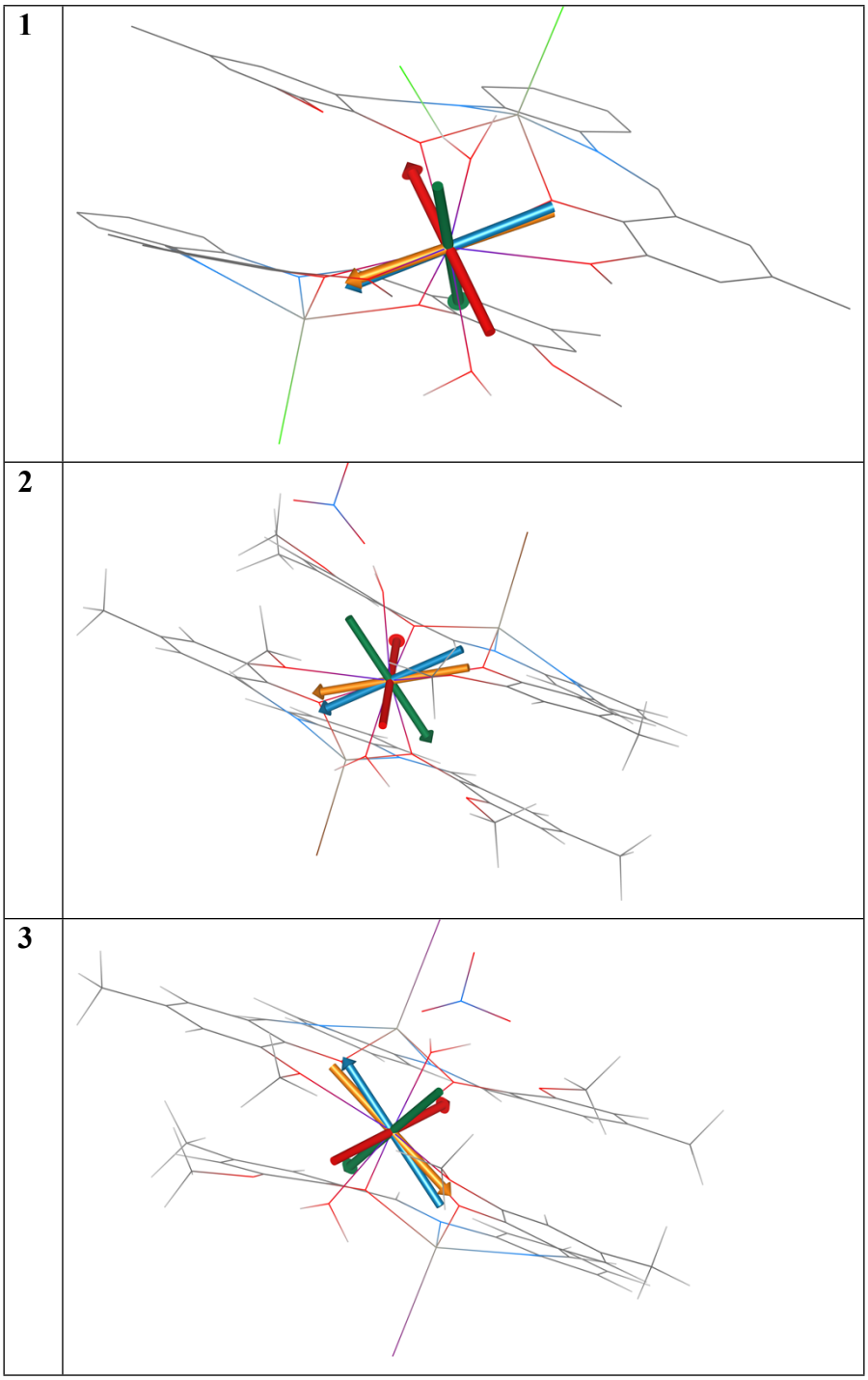


**Fig. S14**. The molecular structures of **1-3** derived from the experimental X-ray geometry used for CASSCF calculations overlaid with of *g*-tensor of the first Kramers doublet (x/y/z-axis are showed as red/green/blue arrows). The magnetic anisotropy axis calculated by Magellan is showed as an orange arrow.

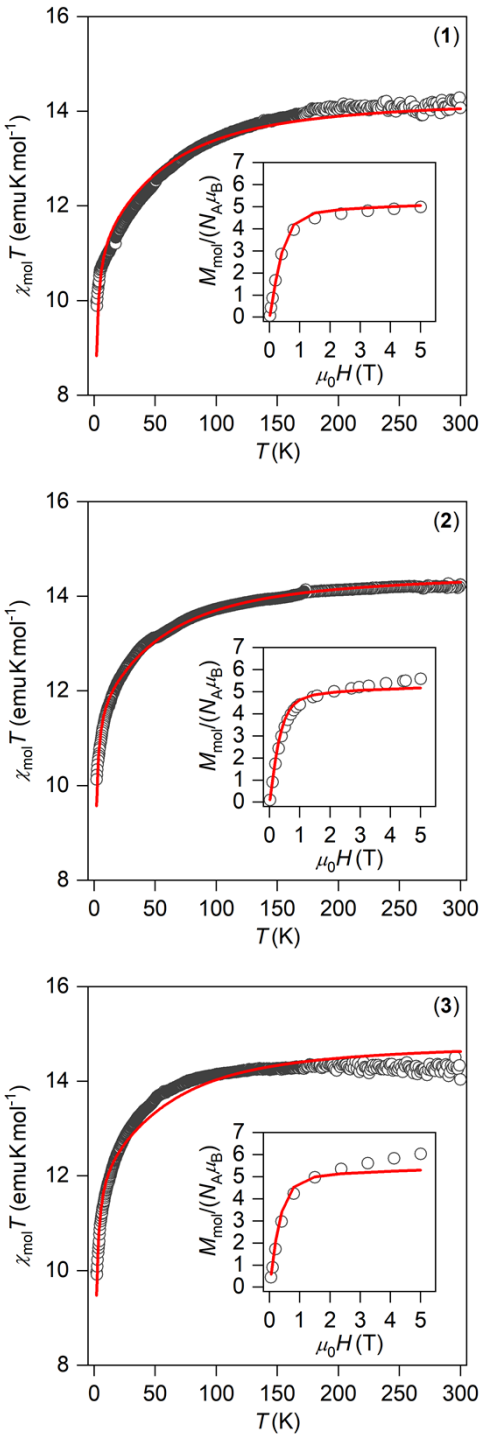


**Fig. S15**. The fits of experimental magnetic data of **1-3** utilizing CASSCF calculations, SINGLE_ANISO program and homemade routine. The best-fitted parameters: $zJ$ = -0.0755 cm$^{-1}$ with scaling coefficient 1.018 for **1**, $zJ$ = -0.0588 cm$^{-1}$ with scaling coefficient 1.036 for **2**, $zJ$ = -0.0718 cm$^{-1}$ with scaling coefficient 1.059 for **3**.